Journal of Chromatography A, xxx (2016) xxx–xxx

Contents lists available at ScienceDirect

Journal of Chromatography A

journal homepage: www.elsevier.com/locate/chroma

Development of zirconia nanoparticles-decorated calcium alginate hydrogel fibers for extraction of organophosphorous pesticides from water and juice samples: Facile synthesis and application with elimination of matrix effects

Maryam Zare[a,b], Zahra Ramezani[a,b], Nadereh Rahbar[a,b,*]

[a] Nanotechnology Research Center, Faculty of Pharmacy, Ahvaz Jundishapur University of Medical Sciences, Ahvaz, Iran
[b] Medicinal Chemistry Department, Faculty of Pharmacy, Ahvaz Jundishapur University of Medical Sciences, Ahvaz, Iran

ARTICLE INFO

Article history:
Received 1 August 2016
Received in revised form 16 October 2016
Accepted 26 October 2016
Available online xxx

Keywords:
Zirconia nanoparticles
Alginate
Organophosphorous pesticides
Micro solid phase extraction
Gas chromatography

ABSTRACT

In this research, novel zirconia nanoparticles-decorated calcium alginate hydrogel fibers (ZNCAHF) were synthesized through a simple, green procedure. ZNCAHF were used as an adsorbent in the micro–solid-phase extraction (MSPE) of methyl parathion (MP), fenitrothion (FT) and malathion (MT) as model pesticides prior to gas chromatography-mass spectroscopic detection (GC–MS). The composition and morphology of the prepared fiber were characterized by Fourier transform-infrared spectroscopy (FTIR), field emission scanning electron microscopy (FESEM), energy dispersive X-ray diffraction (EDX), and differential scanning calorimetry (DSC). Various parameters affecting fabrication of the fiber (weight ratio of components) and relative extraction recovery (pH, amount of adsorbent, extraction time, salt addition, and desorption conditions) were investigated and optimized. Under optimized conditions, the calibration curves were obtained in the concentration range of 0.01–500 ng mL^{-1} with regression coefficients between 0.9997 and 0.9999. The limits of detection (LOD) (S/N = 3) and limits of quantification (LOQ) (S/N = 10) of the method ranged from 0.001 to 0.004 ng mL^{-1} and 0.003 to 0.012 ng mL^{-1}, respectively. The intra-day and inter-day relative standard deviations (RSDs) were 2.2–5.9% and 3.2–7.8%, respectively. The applicability of the fabricated adsorbent was investigated by extraction of selected organophosphorous pesticides (OPPs) from real samples of juice and water. The obtained relative recoveries were in the range of 90.6-105.4%, demonstrating elimination of matrix effects which can be attributed to the remarkable affinity of OPPs toward ZNCAHF.

1. Introduction

In general, sample preparation is a key step in the trace analysis of environmental samples. Extraction as a part of sample preparation is necessary prior to any instrumental analysis. Solid phase extraction (SPE) [1] and related new miniaturized techniques such as solid phase micro extraction (SPME) [2], dispersive micro solid phase extraction (DMSPE) [3], micro solid phase extraction (MSPE) [4] and, stir-bar sorptive extraction (SBSE) [5] have been employed for effective cleanup and preconcentration procedures. In these sorbent-based extraction methods the selection of adsorbent plays an important role in analytical techniques; thus, a promising direction of sample preparation is the development of new adsorbents. However, separating sorbent from sample solutions after extraction and elution is a laborious, time-consuming step. Magnetic sorbents [6], stir-bars [7], stir disks [8], encapsulated sorbent in polypropylene membrane bags [9] and fibers with or without modified surfaces [10,11] have been used to overcome these difficulties, because they are easily isolated from matrices.

Alginates (sodium, potassium and ammonium salts of alginic acid) are water-soluble, natural polysaccharides extracted mainly from brown algae. Industrial applications of alginates are based on their gelling, viscosifying and stabilizing characteristics. Alginates are extensively used in biotechnology, medicine and food industries. They are binary, linear copolymers composed from β-D-mannuronic acid (MA) and α-L-guluronic acid (GA) and are known as nontoxic, biodegradable and non-immunogenic biopolymers (Fig. S1). Differences in M/G ratio and block configuration account for the differences in alginate properties and functionality, especially gelling capability and gel strength.The most important

* Corresponding author at: Department of Medicinal Chemistry, Faculty of Pharmacy, Ahvaz Jundishapur University of Medical Sciences, Ahvaz, Iran.
E-mail addresses: n_rahbar2010@ajums.ac.ir, n_rahbar2001@yahoo.com (N. Rahbar).

http://dx.doi.org/10.1016/j.chroma.2016.10.071
0021-9673/

chemical property of alginates is the selective binding of multivalent cations, which is the basis for their sol/gel transition of alginates. A controlled introduction of cross-linking cations such as Cu^{2+}, Ca^{2+} and Ba^{2+} can form stabilized hydrogels with the formation of a three dimensional network (3D-N) [12–16]. Because of their ability to form stable hydrogels, alginates are widely used for the immobilization of different materials, such as algal biomass, microorganisms and enzymes. In entrapment of living cells within Ca-alginate beads, a cell suspension is mixed with a sodium alginate solution, the mixture dripped into a calcium chloride solution and the droplets instantaneously form gel-spheres entrapping the cells in a 3D-N [16]. Typically, alginates with higher calcium contents (between 3 and 10%, w/w) are nearly or totally insoluble, The proportion and sequence of G blocks in alginate affect the mechanical and swelling properties of the gel beads of Ca-alginate ionic cross-links formed because G-blocks are responsible for specific ion binding with multivalent cations [12,16]. Generally, hydrogels made with synthetic and natural polymers usually have porous surfaces, large specific surface areas and strong loading capacity. The swelling property of hydrogels in water allows the free movement of water and solutes through the inner cavities of hydrogels [17,18]. Recently, metal oxides such as TiO_2 and ZrO_2 supported by alginate-based hydrogels have found applications in the analysis of pharmaceuticals and photo-catalytic and adsorption de-pollution of water bodies [14,15,19–22].

Zirconia acts as a hard Lewis acid because of the zirconium (IV) vacant 3d orbital. Lewis acid sites on the surface of zirconia interact strongly with Lewis-based functional groups (e.g., R—SO_3—, R-PO_3— and R—O—O—), creating coordination bonds [23,24]. This inorganic material with high mechanical property is used as biomaterial for hip prosthesis, tooth crown, and dental implants, and is a candidate for new bone restorative R—SO_3^-, R-PO_3^- and R—O—O^- material due to its low toxicity. Recently, zirconia based sorbents are used for DMSPE of pesticide residues in fish and edible oils [25,26]. The use of zirconia nanoparticles (ZNPs) with high surface area, lack toxicity, physicochemical stability over the whole pH range, and selective affinity to phosphorous groups, is an attractive approach for the capture of phosphate groups. Moreover, it has been employed in water treatments and electroanalytical methods [27–33]. However, the small size and possible release into the treated solution restrict their practical applications. Immobilization and encapsulation of nanoparticles with supports such resin, chitosan and alginate have been effectively used to prevent their leakage into the environment [22].

Organophosphorus pesticides (OPPs) are still used extensively throughout the world to improve yield and quality of fruits, grain crops, and vegetables during the entire period of growth [34]. These pesticides are an important contamination source in the environment because of their widespread application, and their residues become a potential threat to human beings. European Union regulations have established maximum residue limits (MRLs) for OPPs in food and water samples in the ranges of 0.01–0.5 mg kg^{-1} and 0.02–0.1 mg L^{-1}, respectively [35]. Therefore, the effective extraction of these pollutants from complex matrices such as food and environmental samples is necessary and often requires extensive clean-up treatments to isolate target analytes from sample interferences. A wide variety of modern miniaturized sample preparation methodologies in various modes such as dispersive liquid-liquid micro extraction (DLLME) [34,35], SPME [36], and magnetic solid phase extraction [37] coupled with chromatographic techniques have been employed to extract and determine the OPPs. The chemical structures of the examined OPPs are illustrated in Fig. S2.

The object of this work was to develop a facile synthesis methodology for zirconia nanoparticle/calcium alginate hydrogel fiber (ZNCAHF) as novel sorbent for OPPs. The fabricated sorbent with skein shape as a selective, green, and more environmentally-friendly sorbent was easily applied for simultaneous micro extraction and determination of methyl parathion (MP), fenitrothion (FT) and malathion (MT) (the three most toxic and widely-used OPPs) as model analytes in water and juice samples in off-line conjugation with gas chromatography-mass detection (GC–MS). The 3D-N Ca-alginate provides a suitable environment for the immobilization of ZNPs as an adsorbent to OPPs as well as the easy mass transfer of analytes into the network. With the aid of this hydrogel fiber, there is no need for centrifugation or filtration techniques or the use of magnetic fields for magnetic adsorbents, because it is a floating, fibrous solid phase which is easily withdrawn from the solution using forceps.

2. Experimental

2.1. Reagents and standards

Certified standards of MP, FT and MT were supplied by Fluka. Stock solutions of these compounds were prepared in methanol at a concentration of 500 mg L^{-1} and were stored at −20 °C. ZNPs were purchased from Inframat Advanced Materials (Farmington, CT, USA). Sodium alginate (SA) from brown algae with an approximate viscosity of 3500 cps was purchased from Sigma. Methanol (MeOH), toluene, *n*-propanol, dichloromethane (DCM), acetone, acetic acid (HOAC), hydrochloric acid (HCl), sodium hydroxide (NaOH), calcium chloride ($CaCl_2$), and sodium chloride (NaCl) were purchased from Merck (Darmstadt, Germany).

2.2. Instrumentation

GC analysis was carried out on an Agilent 7890A instrument (Palo Alto, CA, USA) with split/splitless injection port, and an Agilent 5975C mass detector system were used. The MS detector was operated in electron impact (EI) mode with ionization energy of 70 eV. Helium (99.999%) was used as the carrier gas at a flow rate 1 mL min^{-1}. OPPs were separated on a 30 m × 0.320 μm HP-5 MS column with 0.25 μm film thickness. The GC column temperature was first 70 °C (t = 0 min), then increased to 150 °C by 25 °C min^{-1}, next raised to 180 °C by increments of 3 °C min^{-1}, and finally increased to 200 °C by increments of 1.5 °C min^{-1}. The split/splitless injection port was set at 250 °C and in splitless mode. The GC–MS interface, ion source and quadruple temperatures were set at 280, 230 and 150 °C, respectively. The solvent delay and total run time for analysis were 7 min and 22 min, respectively. For quantitative determination, MS detector was operated in the time-scheduled selected ion monitoring (SIM) mode. Data acquisition was conducted using Chemstation software. Field emission scanning electron microscopy (FESEM) and energy dispersive x-ray diffraction (EDX) were used to show the morphology, dimension and composition of the ZNCAHF (Mira 3-XMU, Germany). FTIR spectrum was recorded by a vertex 70 FTIR spectrometer (Bruker, Germany). Differential scanning calorimetric (DSC) analysis was performed using a DSC1 STAR system (Mettler Toledo, Switzerland). 10 mg of sample was put in an aluminum pan and heated from 0 to 400 °C at a constant heating rate of 10 °C/min under constant purging of nitrogen at 20 mL/min. Solution pH values were measured by a pH-meter E520 (Metrohm Herisau, Switzerland). Fibers were prepared using a probe sonicator with the power output of 400 w (TOPSONICS, Iran). Solvent desorption of OPPs was performed by an ultrasonic bath (Elma, Germany). All sample solutions were stirred using a CAT M 6.2 magnetic stirrer (Germany).

Please cite this article in press as: M. Zare, et al., Development of zirconia nanoparticles-decorated calcium alginate hydrogel fibers for extraction of organophosphorous pesticides from water and juice samples: Facile synthesis and application with elimination of matrix effects, J. Chromatogr. A (2016), http://dx.doi.org/10.1016/j.chroma.2016.10.071

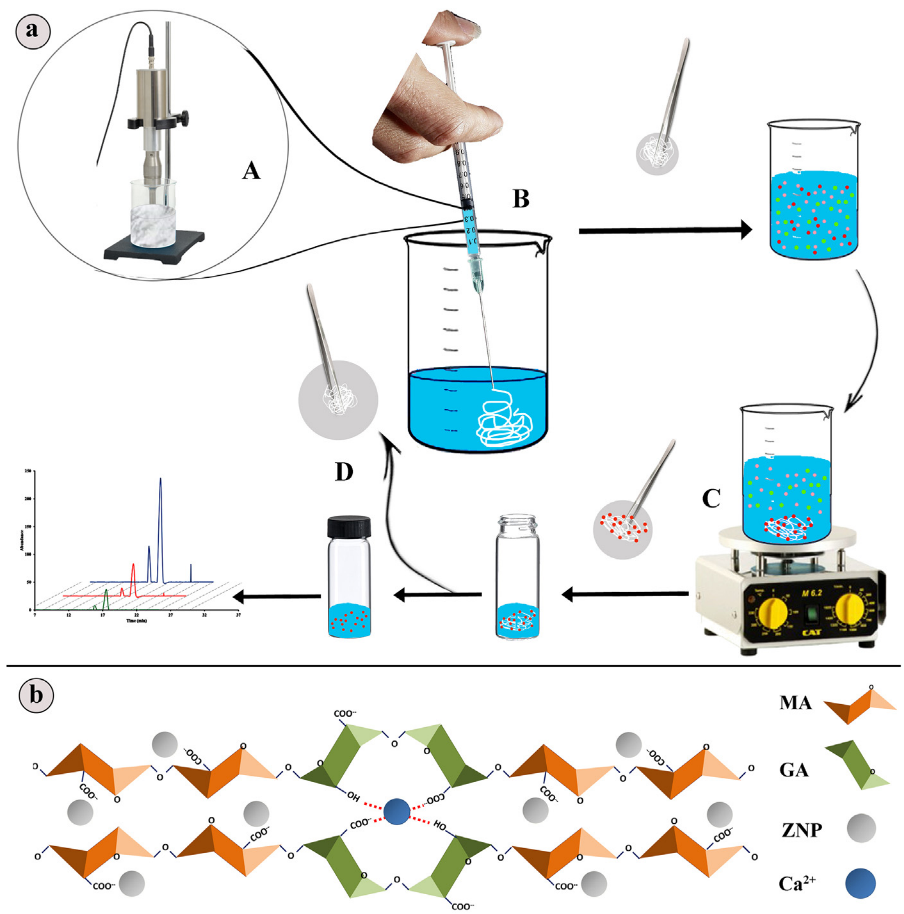

Fig. 1. A schematic illustration of a) adsorbent synthesis steps and MSPE procedure; b) proposed structure for ZNCAHF.

2.3. Synthesis of ZNCAHF

A schematic illustration of the synthesis steps for ZNCAHF is shown in Fig. 1a. The adsorbent was synthesized in two simple steps: preparation of zirconia/sodium alginate suspension, and injection with syringe into the 0.5 mol L^{-1} of $CaCl_2$ solution to form adsorbent fibers. Briefly, first 0.18 g of ZNPs in 20 mL deionized water was sonicated for 10 min to obtain a homogeneous suspension using a probe sonicator. Then, 0.18 g of SA was added into the prepared suspension and sonicated by probe for 10 min to form the homogeneous viscose suspension. 0.5 mL of the prepared suspension was rapidly injected into the $CaCl_2$ solution (0.5 mol L^{-1}) using a grey hub color insulin syringe 27 gauge. As soon as the suspension was injected, the solidified swelled fiber with an approximate weight of 0.1 g (equivalent to 10 mg of dried fiber) appeared. The fiber was easily separated from the $CaCl_2$ solution with forceps, washed with de-ionized water, and dried with a suitable filter paper (Fig. S3).

2.4. Extraction and analysis

The extraction was conducted by immersion of 0.1 g freshly prepared and swelled wet fiber in 5 mL solution containing 0.2 mL acetate buffer (pH 5.5) and an appropriate concentration of standard OPPs solution. The mixture was stirred on a magnetic stirrer at a rate of 500 rpm at room temperature for 5 min. Afterward, the sorbent was easily withdrawn from the solution, washed with de-ionized water to remove any possible interference, and dried with a filter paper. For desorption, the fiber was then inserted inside a small tube and the OPPs were desorbed from the fiber by ultrasound-assisted eluting with 250 μL toluene/DCM (D/T 3:1, v/v) in 10 min using an ultrasonic bath. Finally, a 1 μL aliquot was injected into the GC–MS. The Photographs of the system setup are also presented in the Supplementary data (Fig. S4).

2.5. Analysis of real samples

A river water sample was collected from the Karun River in Ahvaz (Khuzestan province, Iran). A tap water sample was collected from Ahvaz. Mineral water and cherry juice were purchased from local supermarkets in Ahvaz. All samples were filtered through a 0.45 mm membrane filter and stored at 4 °C. Each 5 mL of solution including 2.5 mL of real sample, spiked with standard analytes, and 0.2 mL of acetate buffer (pH 5.5) was subjected to the optimized extraction and analytical method without any pretreatments. Extractions from non-spiked samples were also carried out in parallel. All experiments were performed in triplicate. Relative recovery (R%) was calculated using the following equation:

$$\% = (C_F/C_A) \times 100$$

where C_F, C_A are founded concentrations in the real samples spiked with the known amount of OPPs standard solution and the added concentrations of OPPs in real samples, respectively.

3. Results and discussion

3.1. Characterization of ZNCAHF

FT-IR spectra of ZrO_2, SA and ZNCAHF are illustrated in Fig. 2. As shown in Fig. 2a, the main band at about 508 cm^{-1} is attributed

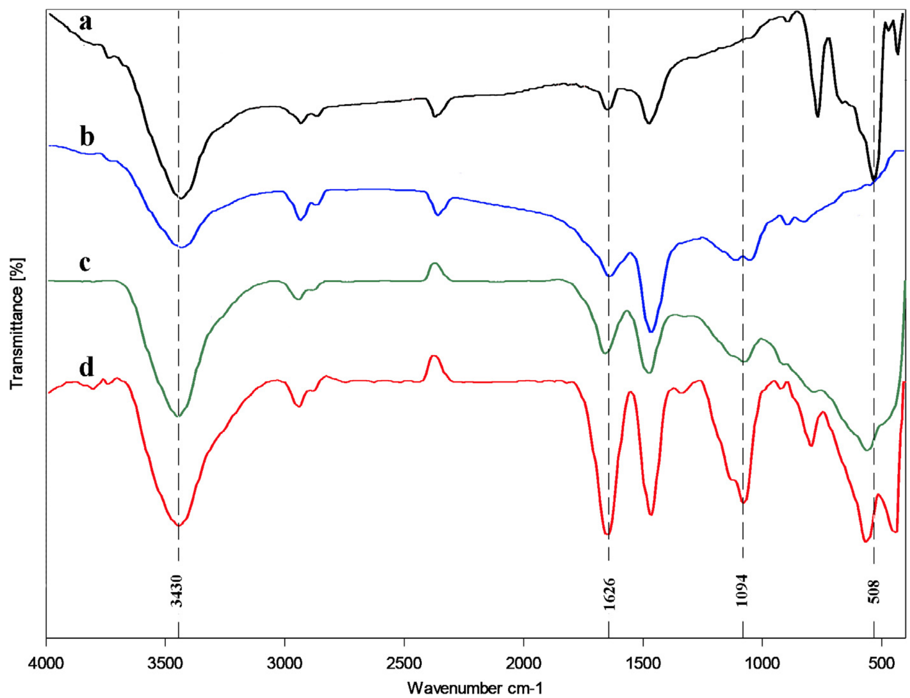

Fig. 2. FT-IR spectra of a) ZNP, b)SA, c) ZNCAHF, d) OPPs-adsorbed ZNCAHF.

to the Zr-O vibration. The other bands around 1631 and 3430 cm^{-1} are ascribed to the bending and stretching vibration of —OH from adsorbed water molecules. SA displayed the absorption peak at 1626 cm^{-1} corresponding to the stretching vibration of the carbonyl group of the carboxylic acid group. The adsorption peaks at 1037 and 1094 are due to the O—H bending vibration of the alcoholic group (surface hydroxyl groups) in SA [19,36]. In addition, the peaks at about 2862 and 2925 cm^{-1} correspond to the symmetric and asymmetric vibration band of the —CH_2 group (Fig. 2b). The spectrum of ZNCAHF shows the Zr-O vibration peak at 510 with a slight shift indicating the interaction between the —COO— groups of AS and zirconia exists (Fig. 2c) [23,24]. The peak observed at 510 cm^{-1} correlated to Zr—O bond in ZNCAHF presented a larger shift to 515 cm^{-1} in the case of OPPs-adsorbed ZNCAHF, indicating the interaction between the analytes and the zirconia constituent of the adsorbent (Fig. 2d).

The morphology and composition of ZNCAHF are illustrated in Fig. 3. The outward appearance of the synthesized adsorbent with continually fibrous shape is shown in Fig. 3a. The FESEM micrographs of the fiber with different magnifications are shown in Fig. 3b and c. Obviously, ZNPs are uniformly immobilized in Ca-alginate 3D-N and although, the zirconia particles have been covered with hydrogel, their sizes are kept in the criteria defined for nano-materials (<100 nm). The EDX results confirmed that ZNPs were successfully impregnated in Ca-alginate 3D-N (Fig. 3d).

DSC thermograms of ZNP, SA and ZNCAHF are shown in Fig. 4. The DSC curve of ZNP exhibited an endothermic weak peak at about 100 °C that can be correlated to the loose water bonded on the zirconia surface (Fig. 4a). As seen in Fig. 4b, the DSC profile of SA displays an endothermic peak at about 160 °C that, probably because of the loss of water, linked to the —COO— groups (hydrophilic groups of biopolymer) and the melting of crystalline structure [38], while two intense exothermic peaks at 240 °C and 370 °C are correlated to pyrolysis (biopolymer degradation) and oxidation reactions, respectively [39–42]. The data presented in Fig. 4c clearly shows that the peak attributed to the pyrolysis reaction was weakened and the oxidation peak was disappeared suggesting that ZNCAHF has become more stable comparing to SA in the temperatures ranged from 0 to 400 °C. This phenomenon can be explained by the interaction of alginate with the metals (calcium and zirconium) leading to the stabilization of the biopolymer in high temperatures probably due to an increase in cross-linking density that restrict the molecular mobility, and the role of ZNPs as thermal barrier [20,42,43]. Moreover, the endothermic peak at about 150 °C in the case of SA appeared as a much stronger peak in the thermogram of ZNCAHF. This observation might be attributed to enhanced chain stiffness due to the crosslinking with Ca^{2+} and the bonded ZNPs to —COO— groups in ZNCAHF and clearly shows that the metals (calcium and zirconium) could affect the physicochemical characters of the adsorbent [24,44,45].

3.2. *Optimization of experimental conditions*

In order to obtain the best of ZNCAHF, various parameters affecting adsorption efficiency such as ZrO_2/Alginate ratio, pH, the amount of sorbent, extraction time and type, composition and volume of desorption solvents, and sonication time, in the desorption step were optimized.

3.2.1. *ZNCAHF composition*

To obtain the most sensitive and fragmentation-resistant fiber, different weight compositions (80:20, 70:30, 60:40, 50:50, 40:60, 30:70 and 20:80) of ZNP:SA were synthesized. The constructed fibers were subjected to the extraction procedure, and the best quality of fiber and extraction recovery was obtained by 50:50 (w/w) ratios. The fibers with ZNP ratios of more than 50% by weight showed fragmentation when stirred with sample solution, and the adsorbent could not be easily separated. Extraction efficiency was slightly decreased proportional to the decrease in ZNP ratio (less than 50%), indicating the role of ZNPs as adsorbing sites in ZNCAHF. The ZNP could be strongly retained by hydrogel without leakage in the stirring and sonication steps, suggesting the possible bonding of ZNPs to —COO— groups in M-blocks of alginate [24]. Therefore, it can be suggested that G-blocks in AS may selectively bind with Ca^{2+} ions and M-blocks are free for possible bonding with zirconia as depicted in Fig. 1b [16].

Please cite this article in press as: M. Zare, et al., Development of zirconia nanoparticles-decorated calcium alginate hydrogel fibers for extraction of organophosphorous pesticides from water and juice samples: Facile synthesis and application with elimination of matrix effects, J. Chromatogr. A (2016), http://dx.doi.org/10.1016/j.chroma.2016.10.071

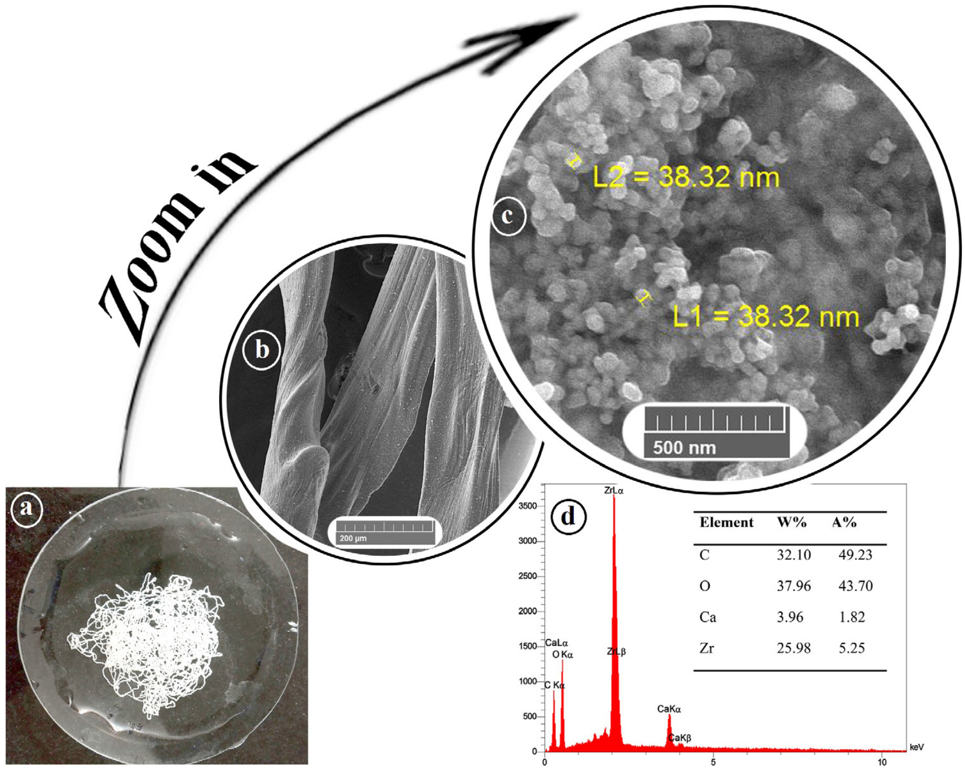

Fig. 3. The morphology and composition of ZNCAHF: a) The outward appearance, b and c) The FESEM image with different magnifications, d) The EDX spectra.

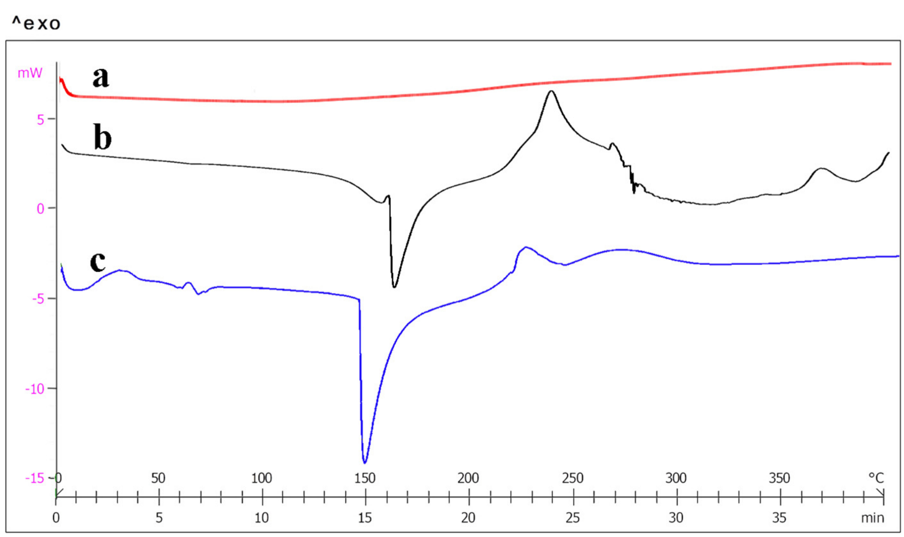

Fig. 4. The DSC curves of a) ZNP, b) SA, c) ZNCAHF.

3.2.2. Effect of pH

The stability, charge and adsorption characteristics of adsorbent toward analytes as well as the chemical properties of analytes can be affected by the pH of the solution. Hence, the effect of pH on the adsorption of the selected OPPs was studied over the range of 2–9 using sodium hydroxide and hydrochloric acid solutions. The results shown in Fig. 5a indicate that the pH of the sample solution influenced extraction efficiency. In pH values lower than 5 and higher than 6, the extraction recovery of all OPPs decreased and in pHs 5–6 the peak areas remained almost constant. Zirconia is known as a Lewis acid, and the adsorption of OPPs on the ZNCAHF surface can be explained by the attraction between vacant 3d orbital of Zr(IV) and free electron pairs of phosphate moiety in the OPPs neutral molecules. At a pH between 5 and 6, the best extraction recovery was achieved, because the surface of the adsorbent is neutral and Lewis acid-base attraction occurred between zirconia and the phosphate moiety of OPPs. However, since zirconia is an amphoteric metal oxide with an isoelectric point of 5.7, its surface behaves like a brönsted acid or base [24,27,46,47]. Thus, in pH values lower and higher than the isoelectric point of zirconia, the Lewis acid-base attraction between ZNCAHF and OPPs weakens and extraction efficiency decreases. Moreover, in a pH lower than 3, slight leakage of ZNP from ZNCAHF was observed. As mentioned in section 3.2.1, zirconia might be retained in AS via carboxcylate groups. In a pH lower 3, these functional groups are in protonated forms due to their dissociation constants (pKa MA = 3.38 and pKa

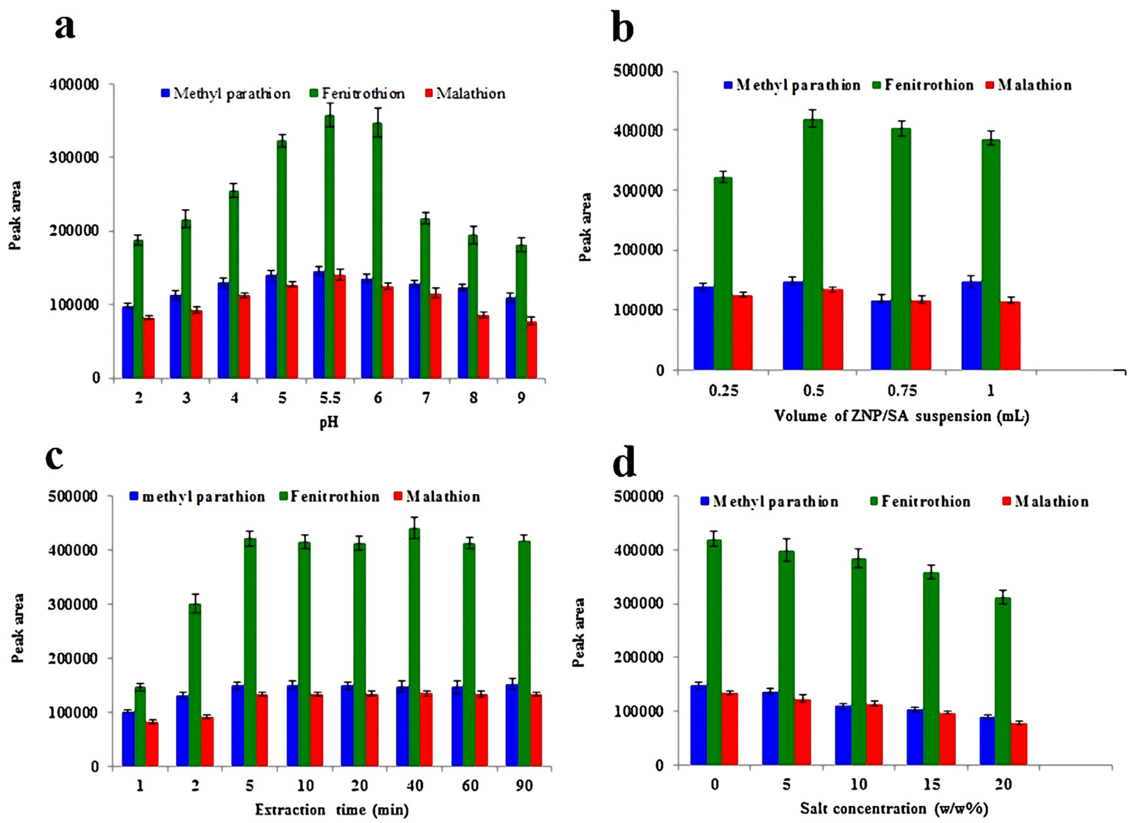

Fig. 5. Effects of a) pH (conditions: 5 mL of OPPs solution, 0.1 μg mL^{-1}; extraction time, 10 min; fiber suspension, 0.25 mL; eluting solvent, 0.5 mL of methanol; sonication time for desorption of analytes, 10 min), b) the amount of ZNCAHF (conditions: 5 mL of OPPs solution, 0.1 μg mL^{-1}; pH, 5.5; extraction time, 10 min; eluting solvent, 0.5 mL of methanol; sonication time for desorption of analytes, 10 min), c) extraction time (conditions: 5 mL of OPPs solution, 0.1 μg mL^{-1}; pH, 5.5; fiber suspension, 0.5 mL; eluting solvent, 0.5 mL of methanol; sonication time for desorption of analytes, 10 min), and d) salt concentration on the extraction efficiency (conditions: 5 mL of OPPs solution, 0.1 μg mL^{-1}; pH, 5.5; extraction time, 5 min; fiber suspension, 0.5 mL; eluting solvent, 0.5 mL of methanol; sonication time for desorption of analytes, 10 min).

GA = 3.65) and zirconia cannot bind with −**COO**$^{-}$OO− groups [48]. Therefore, in the remaining experiments, the pH of the sample solutions was adjusted to 5.5 using 0.2 mL of acetate buffer. The effect of buffer volume on extraction is shown in Fig. S5. The buffer volume had no significant effect on the peak areas of the extracted OPPs.

3.2.3. Effect of ZNCAHF amount

To achieve the highest possible extraction efficiency, the effect of the fiber amount was studied by injecting the ZNP/SA suspension in the range of 0.25–1 mL into the $CaCl_2$ solution. Extraction efficiency was increased from 0.25 to 0.5 mL of ZNP/SA suspension, and remained almost constant in higher volumes. Therefore, 0.5 mL of suspension was selected to produce the best amount of fiber (Fig. 5b).

3.2.4. Effect of extraction time

Extraction time refers to the period allowed for the partition of analyte between solution and adsorbent. To achieve higher relative extraction recovery, extraction times in the range of 1–90 min were examined by shaking the sample solution on a magnetic stirrer at 500 rpm. As shown in Fig. 5c, the peak areas increased slightly up to 5 min, while no improvement on the relative extraction recovery was observed at higher extraction times; therefore, the extraction time of 5 min was chosen as the optimum value. The results indicated that the adsorption kinetics is very fast, and the adsorption process reached equilibrium in a short time.

3.2.5. Effect of salt concentration

The addition of salt to the aqueous solution may improve extraction recovery because of the salting-out effect. Therefore, different amounts of NaCl ranging 0–20% (w/v) were added into the sample solutions to check the effect of salt concentration. As shown in Fig. 5d, the amount of extracted analytes was reduced by the addition of salt. This can be due to the fact that the existence of salt increases the viscosity of the sample solution, resulting in a reduction in the mass transfer of OPPs from the aqueous phase to the adsorbent surface [37,49]. Considering these results and the simplicity of the extraction procedure, further experiments were performed without adding salt.

3.2.6. Desorption conditions

Selecting suitable conditions, such as type and volume of eluting solvent, and desorption time for effective desorption of the analytes from the adsorbent, is the key step in every MSPE procedure. The proper selection of eluting solvent can lead to a better desorption of analytes from the adsorbent resulting in higher efficiency. Hence, desorption studies were performed using different organic solvents including methanol, acetone, DCM, *n*-propanol and toluene and their mixtures. As illustrated in Fig. 6a, the desorption ability of the mixture of toluene and DCM (T/D 3:1 v/v) was better than that of other solvents. The effect of selected solvent volume on the extraction efficiency of the examined OPPs was also investigated. It was found that the analytes could be effectively desorbed by 250 μL of a mixture of toluene and DCM (Fig. 6b). In order to achieve the best sonication time in desorbing, different times in the range of 2–20 min were studied. The best sonication time was found to be 10 min as shown in Fig. 6c.

Table 1
Analytical features for determination of OPPs by the proposed MSPE/GC–MS method.

Pesticide	LOD[a]	LOQ[b]	LDR[c]	R^2[d]	Regression equation
Methyl parathion	0.003	0.010	0.01–500	0.9999	y = 2307.8 x + 6.8534
Fenitrothion	0.001	0.003	0.01–250	0.9997	y = 5019.3 x + 7.3589
Malathion	0.004	0.012	0.01–500	0.9998	y = 2025.2 x + 7.5332

[a] Limit of detection (ng mL^{-1}).
[b] Limit of quantification (ng mL^{-1}).
[c] Linear dynamic range (ng mL^{-1}).
[d] Regression coefficient.

Table 2
Relative recoveries and RSDs of OPPs on three spiked standard levels.

Pesticide	Added[a]	Found[b]	Recovery[c]	RSD[d]	
				Intra-day (n = 5)	Inter-day (n = 3)
Methyl parathion	5.0	5.3	106.9	5.2	7.4
	50.0	47.5	94.9	3.5	4.2
	250.0	247.9	99.2	2.2	3.7
Fenitrothion	5.0	5.3	105.0	4.3	6.5
	50.0	50.3	100.5	2.6	5.4
	250.0	249.1	99.7	2.3	3.2
Malathion	5.0	5.1	101.6	5.9	7.8
	50.0	47.4	94.7	4.0	4.6
	250.0	253.0	101.2	2.7	4.2

[a] Spiked concentrations of MP, FT and MT (μg L^{-1}).
[b] Recovered concentrations of MP, FT and MT (μg L^{-1}) (n = 5).
[c] Relative recovery (%).
[d] Relative standard deviations (%).

Table 3
Investigation of matrices effect in spiked real samples with the proposed method (all samples were diluted with deionized water at a ratio of 1:2).

Sample		MP		FT		MT	
	Added[a]	Found[b]	Recovery[c]	Found	Recovery	Found	Recovery
River water	–	ND[d]	–	ND	–	ND	–
	25.0	24.1	96.5	23.8	95.2	22.9	91.5
	100.0	91.9	91.9	97.9	97.9	101.4	101.4
	250.0	243.1	97.2	238.6	95.4	234.7	93.9
Tap water	–	ND	–	ND	–	ND	–
	25.0	25.3	101.1	23.5	94.2	26.0	104.0
	100.0	93.4	93.4	101.1	101.1	97.1	97.1
	250.0	252.8	101.1	242.5	97.0	240.7	96.3
Mineral water	–	ND	–	ND	–	ND	–
	25.0	26.1	104.4	24.7	98.7	24.8	99.3
	100.0	96.9	96.9	96.8	96.8	103.4	103.4
	250.0	258.9	103.5	251.3	100.5	241.5	96.6
Cherry juice	–	ND	–	ND	–	ND	–
	25.0	22.7	90.6	23.4	93.6	23.0	92.1
	100.0	97.6	97.6	95.5	95.5	105.4	105.4
	250.0	235.8	94.3	262.5	105.0	230.6	92.2

[a] Spiked concentrations of MP, FT and MT (μg L^{-1}).
[b] Recovered concentrations of MP, FT and MT (μg L^{-1}).
[c] Relative recovery (%).
[d] Not detected.

Table 4
Comparison of the current method with recent reported methods for the determination of OPPs.

Method	Matrices	LDR (μg L^{-1})	LODs (μg L^{-1})	Extraction time(min)	Recovery (%)	Adsorbent (mg)	References
MSPE-GC-NPD	Fruit juice	0.003–50	0.001–0.005	2	86–107	10	[50]
CNESE[a]-UHPLC-MS	Ginseng	0.5–500	00.08–0.29	15	82–110	1000	[51]
SBSE[b]-GC-FPD	Water	0.2–100	0.043–0.085	25	80–115	–	[52]
ET-DLLME[c]-GC-FID	Water- fruit juice	2.60–1000	0.82–2.72	9	64–83	–	[35]
MSPE-GC–MS	Water	100–20,000	0.1–10.30	30	87–112	1	[53]
MSPE-GC–MS	Water- fruit juice	0.01–500	0.001–0.004	5	90–105	10	Present work

[a] Carbon nanotube envelope-based solvent extraction.
[b] Stir bar sorptive extraction.
[c] Elevated temperature–dispersive liquid–liquid microextraction.

Please cite this article in press as: M. Zare, et al., Development of zirconia nanoparticles-decorated calcium alginate hydrogel fibers for extraction of organophosphorous pesticides from water and juice samples: Facile synthesis and application with elimination of matrix effects, J. Chromatogr. A (2016), http://dx.doi.org/10.1016/j.chroma.2016.10.071

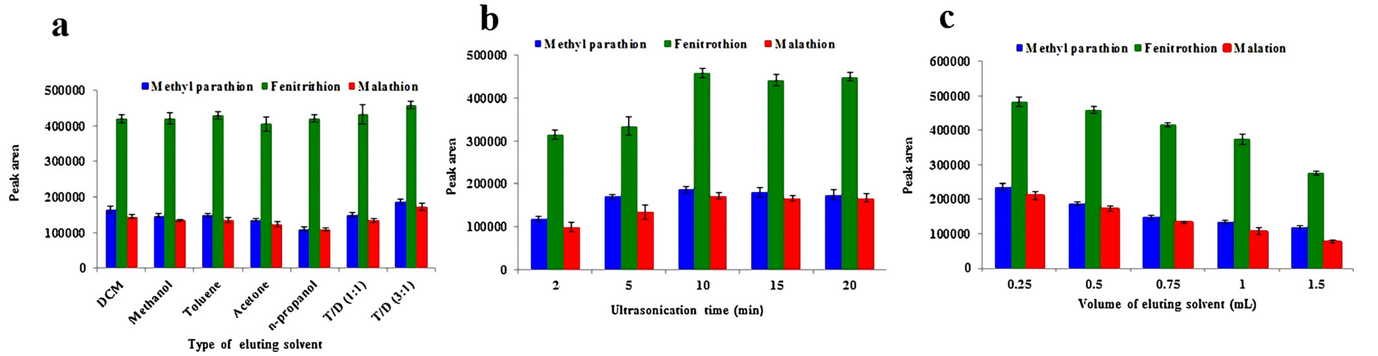

Fig. 6. Optimization of desorption conditions: a) type of eluting solvent (conditions: 5 mL of OPPs solution, 0.1 μg mL^{-1}; pH, 5.5; extraction time, 5 min; fiber suspension, 0.5 mL; volume of eluting solvent, 0.5 mL; sonication time for desorption of analytes, 10 min), b) volume of eluting solvent, c) Effect of sonication time in desorption.

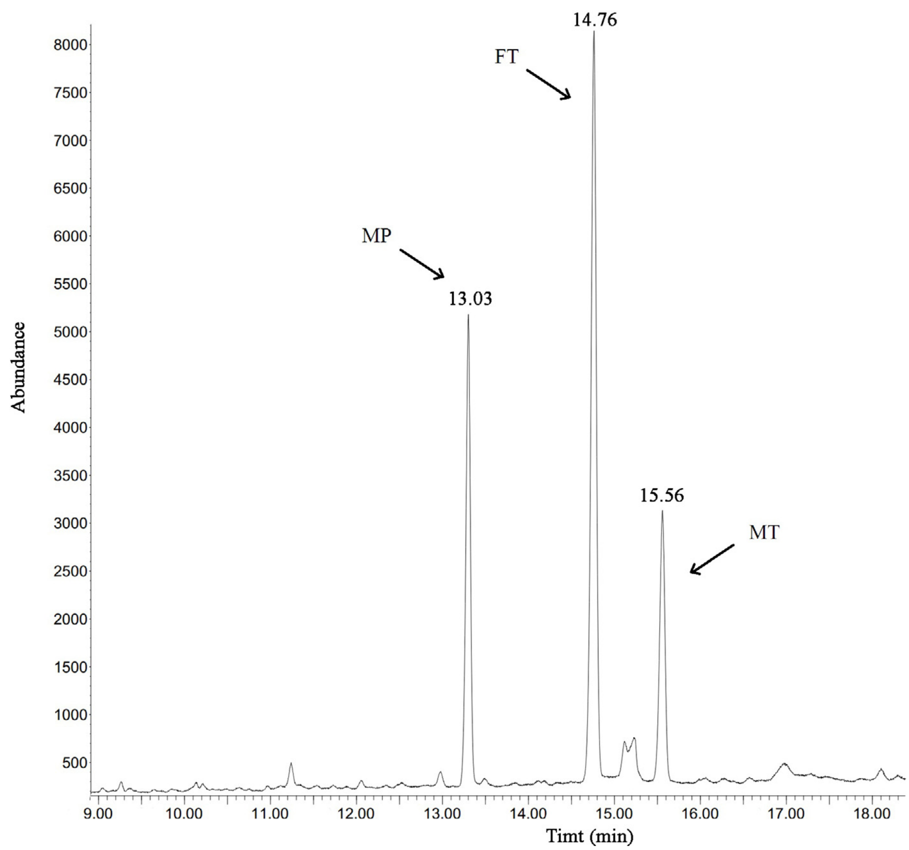

Fig. 7. A typical chromatogram of a cherry juice sample after being spiked with OPPs at 100 ng mL^{-1}.

3.3. Analytical performance and method validation

In order to show the validation of the proposed method, the analytical features of the method such as dynamic range of the calibration curve, LOD, LOQ, accuracy and precision were examined. A series of sample solutions containing MP, FT and MT in the range of 0.01–500 ng mL^{-1} at ten selected concentration levels was prepared and analyzed under optimal extraction conditions. All obtained data were the averages of three determinations. Then, the calibration curves of OPPs were constructed using least squares linear regression method. The limits of detection (LODs) and quantification (LOQs) of the method were determined at signal to noise ratio of 3 and 10 by injecting a series of samples with known concentration, respectively. The analytical features of the method are given in Table 1. The peak area measurements of analyte solution containing the quality control (QC) amounts of OPPs were interpolated from the calibration curve on the same day to give concentrations of the analyte. The results from QC samples in five runs on the same day and on three consecutive days were used to evaluate the precision and accuracy of the developed method. To evaluate the intra- and inter-day precision of the developed method, showing the reproducibility and repeatability terms, five similar experiments were performed for the QC samples at concentration levels of 5, 50 and 250 ng mL^{-1} on the same day and on three consecutive days. As can be seen in Table 2, the RSD% results ranged from 2.2% to 5.9% for analysis of intra-day spiked samples, revealing the high reproducibility of the proposed method. Moreover, the inter-day precision results were between 3.2% and 7.8%.

3.4. Application of the method to water and juice samples

The optimized analytical procedure was applied to analyze water and juice samples to show the applicability of the proposed method for real samples. The results are shown in Table 3. The extraction recoveries from water and juice real sample solutions containing low, middle and high concentrations of MP, FT and MT (25, 100 and 250 ng mL^{-1}) were in the range of 90.6–105.4%. All investigated real samples met the criteria for matrix effect (70–120%) according to the guidance document on analytical quality control and validation procedures for pesticide residues analysis in food and feed [50]. Therefore, no significant matrix effect for MSPE of the selected OPPs by ZNCAHF was observed in various matrices, indicating that the use of matrix-matched calibration standards is not required. The typical chromatogram of a cherry juice sample after being spiked with OPPs at 100 ng mL^{-1} is shown in Fig. 7.

4. Conclusion

In this work a new and simple method was developed to prepare a selective and green adsorbent fiber based on the formation of three dimensional hydrogel by SA and Ca^{2+} ions and immobilization of ZNPs in the network, and reported for first time. The modification of Ca-alginate hydrogel with ZNPs led to the fabrication of a sorbent with a high surface area that possesses plenty of sites for – adsorption of OPPs. The fabricated adsorbent was resistant to ZNP leakage in the solution stirring and sonication steps. With the aid of ZNCAHF the MSPE procedure carried out without limitation due to the isolation of adsorbent from sample solution and desorption solvent. Ease of separation from solution and having high specific area due to its thin fibrous shape and ZNPs content are two essential features of the synthesized fiber. Most importantly, the fiber showed high selectivity to the OPPs and almost no matrix interference was observed. Therefore, satisfactory recoveries from real samples were obtained, indicating the potential of the synthesized fiber for selective and sensitive detection of OPPs in complicated matrices. Some analytical features of the current method and other recent methods for the extraction and determination of OPPs are compared in Table 4. As shown, the proposed method possesses a wide dynamic range, low LODs, short extraction time, and satisfactory recoveries compared with most of the other reported methods, which could be related to the great adsorptive ability of ZNCAHF toward OPPs. The results revealed that the synthesized adsorbent can be applied in a simple, fast, and effective MSPE procedure for OPPs extraction from various matrices. In addition, the proposed procedure can be applied for the synthesis of fibers other than ZNCAHF with various modifying compounds providing an excellent prospective in the fabrication of selective solid phases without the need for separation methods (filtration and centrifugation) or even the application of magnetic sorbents which are generally nonselective adsorbents.

Acknowledgement

The authors gratefully acknowledge the financial support provided by the Research Council of Ahvaz Jundishapur University of Medical Sciences and Nanotechnology Research Center under grant number GP 94109. This paper is extracted from Miss Zare's thesis.

Appendix A. Supplementary data

Supplementary data associated with this article can be found, in the online version, at http://dx.doi.org/10.1016/j.chroma.2016.10.071.

References

[1] C. Qi, Q. Cai, P. Zhao, X. Jia, N. Lu, L. He, X. Hou, The metal-organic framework MIL-101(Cr) as efficient adsorbent in a vortex-assisted dispersive solid-phase extraction of imatinib mesylate in rat plasma coupled with ultra-performance liquid chromatography/mass spectrometry: application to a pharmacokinetic study, J. Chromatogr. A 1449 (2016) 30–38.
[2] K. Korba, L. Pelit, F.O. Pelit, K.V. Özdokur, H. Ertaş, A.E. Eroğlu, F.N. Ertaş, Preparation and characterization of sodium dodecyl sulfate doped polypyrrole solid phase micro extraction fiber and its application to endocrine disruptor pesticide analysis, J. Chromatogr. B 929 (2013) 90–96.
[3] A.A. Asgharinezhad, H. Ebrahimzadeh, F. Mirbabaei, N. Mollazadeh, N. Shekari, Dispersive micro-solid-phase extraction of benzodiazepines from biological fluids based on polyaniline/magnetic nanoparticles composite, Anal. Chim. Acta 844 (2014) 80–89.
[4] Z. Huang, H.K. Lee, Micro-solid-phase extraction of organochlorine pesticides using porous metal-organic framework MIL-101 as sorbent, J. Chromatogr. A 1401 (2015) 9–16.
[5] A. Guart, I. Calabuig, S. Lacorte, A. Borrell, Continental bottled water assess-ment by stir bar sorptive extraction followed by gas chromatography-tandemmass spectrometry (SBSE-GC–MS/MS), Environ. Sci. Pollut. Res. 21 (2014) 2846–2855.
[6] F. Makkliang, P. Kanatharana, P. Thavarungkul, C. Thammakhet, Development of magnetic micro-solid phase extraction for analysis of phthalate esters in packaged food, Food Chem. 166 (2015) 275–282.
[7] J. Płotka-Wasylka, N. Szczepańska, M. de la Guardia, J. Namieśnik, Miniaturized solid-phase extraction techniques, TrAC Trends Anal. Chem. 73 (2015) 19–38.
[8] M. Roldán-Pijuán, R. Lucena, S. Cárdenas, M. Valcárcel, Micro-solid phase extraction based on oxidized single-walled carbon nanohorns immobilized on a stir borosilicate disk: application to the preconcentration of the endocrine disruptor benzophenone-3, Microchem. J. 115 (2014) 87–94.
[9] N.N. Naing, S.F.Y. Li, H.K. Lee, Magnetic micro-solid-phase-extraction of polycyclic aromatic hydrocarbons in water, J. Chromatogr. A 1440 (2016) 23–30.
[10] A.M. Filho, F.N. dos Santos, P.A.d.P. Pereira, Development, validation and application of a method based on DI-SPME and GC–MS for determination of pesticides of different chemical groups in surface and groundwater samples, Microchem. J. 96 (2010) 139–145.
[11] Y.-L. Wang, Y.-L. Gao, P.-P. Wang, H. Shang, S.-Y. Pan, X.-J. Li, Sol-gel molecularly imprinted polymer for selective solid phase microextraction of organophosphorous pesticides, Talanta 115 (2013) 920–927.
[12] Y.-G. Liu, X.-J. Hu, H. Wang, A.-W. Chen, S.-M. Liu, Y.-M. Guo, Y. He, X. Hu, J. Li, S.-H. Liu, Y.-q. Wang, L. Zhou, Photoreduction of Cr(VI) from acidic aqueous solution using TiO_2-impregnated glutaraldehyde-crosslinked alginate beads and the effects of Fe(III) ions, Chem. Eng. J. 226 (2013) 131–138.
[13] G. Mollica, F. Ziarelli, S. Lack, F. Brunel, S. Viel, Characterization of insoluble calcium alginates by solid-state NMR, Carbohydr. Polym. 87 (2012) 383–391.
[14] S.K. Papageorgiou, F.K. Katsaros, E.P. Favvas, G.E. Romanos, C.P. Athanasekou, K.G. Beltsios, O.I. Tzialla, P. Falaras, Alginate fibers as photocatalyst immobilizing agents applied in hybrid photocatalytic/ultrafiltration water treatment processes, Water Res. 46 (2012) 1858–1872.
[15] S. Sarkar, S. Chakraborty, C. Bhattacharjee, Photocatalytic degradation of pharmaceutical wastes by alginate supported TiO_2 nanoparticles in packed bed photo reactor (PBPR), Ecotoxicol. Environ. Saf. 121 (2015) 263–270.
[16] K.I. Draget, C. Taylor, Chemical, physical and biological properties of alginates and theirbiomedical implications, Food Hydrocol. 25 (2011) 251–256.
[17] J. Jiang, Y. Chen, W. Wang, B. Cui, N. Wan, Synthesis of superparamagnetic carboxymethyl chitosan/sodium alginate nanosphere and its application for immobilizing α-amylase, Carbohydr. Polym. 151 (2016) 600–605.
[18] I. Pajic-Lijakovic, S. Levic, M. Hadnađev, Z. Stevanovic-Dajic, R. Radosevic, V. Nedovic, B. Bugarski, Structural changes of Ca-alginate beads caused by immobilized yeast cell growth, Biochem. Eng. J. 103 (2015) 32–38.
[19] S.K. Swain, T. Patnaik, P.C. Patnaik, U. Jha, R.K. Dey, Development of new alginate entrapped Fe(III)–Zr(IV) binary mixed oxide for removal of fluoride from water bodies, Chem. Eng. J. 215–216 (2013) 763–771.
[20] A. Konwar, A. Gogoi, D. Chowdhury, Magnetic alginate–Fe_3O_4 hydrogel fiber capable of ciprofloxacin hydrochloride adsorption/separation in aqueous solution, RSC Adv. 5 (2015) 81573–81582.
[21] E. Pabjańczyk-Wlazło, G. Szparaga, P. Król, E. Skrzetuska, K. Wojtasik, M. Sieradzka, M. Boguń, S. Rabiej, Sodium alginate fibers containing nanosilver, Adv. Polym. Tech. 33 (2014) 21450.
[22] O.-H. Kwon, J.-O. Kim, D.-W. Cho, R. Kumar, S.H. Baek, M.B. Kurade, B.-H. Jeon, Adsorption of As(III), As(V) and Cu(II) on zirconium oxide immobilized alginate beads in aqueous phase, Chemosphere 160 (2016) 126–133.
[23] J. Dai, X. Yang, P.W. Carr, Comparison of the chromatography of octadecyl silane bonded silica and polybutadiene-coated zirconia phases based on a diverse set of cationic drugs, J. Chromatogr. A 1005 (2003) 63–82.
[24] A. Lozano, Ł. Rajski, S. Uclés, N. Belmonte-Valles, M. Mezcua, A.R. Fernández-Alba, Evaluation of zirconium dioxide-based sorbents to decrease the matrix effect in avocado and almond multi residue pesticide analysis followed by gas chromatography tandem mass spectrometry, Talanta 118 (2014) 68–83.
[25] X.T. Peng, L. Jiang, Y. Gong, X.Z. Hu, L.J. Peng, Y.Q. Feng, Preparation of mesoporous ZrO_2-coated magnetic microsphere and its application in the

multi-residue analysis of pesticides and PCBs in fish by GC–MS/MS, Talanta 132 (2015) 118–125.
[26] T. Tuzimski, T. Rejczak, Application of HPLC-DAD after SPE/QuEChERS with ZrO_2-based sorbent in d-SPE clean-up step for pesticide analysis in edible oils, Food Chem. 190 (2016) 71–79.
[27] H. Jiang, P. Chen, S. Luo, X. Tu, Q. Cao, M. Shu, Synthesis of novel nanocomposite Fe_3O_4/ZrO_2/chitosan and its application for removal of nitrate and phosphate, Appl. Surf. Sci. 284 (2013) 942–949.
[28] J. Gong, X. Miao, H. Wan, D. Song, Facile synthesis of zirconia nanoparticles-decorated graphene hybrid nanosheets for an enzymeless methyl parathion sensor, Sens. Actuators B 162 (2012) 341–347.
[29] H. Liu, X. Sun, C. Yin, C. Hu, Removal of phosphate by mesoporous ZrO_2, J. Hazard. Mater. 151 (2008) 616–622.
[30] T.J. Matsumoto, S.H. An, T. Ishimoto, T. Nakano, T. Matsumoto, S. Imazato, Zirconia-hydroxyapatite composite material with micro porous structure, Dent. Mater. 27 (2011) e205–212.
[31] M. Wang, Z. Li, Nano-composite ZrO_2/Au film electrode for voltammetric detection of parathion, Sens. Actuators B 133 (2008) 607–612.
[32] E. Zong, D. Wei, H. Wan, S. Zheng, Z. Xu, D. Zhu, Adsorptive removal of phosphate ions from aqueous solution using zirconia-functionalized graphite oxide, Chem. Eng. J. 221 (2013) 193–203.
[33] H. Parham, N. Rahbar, Square wave voltammetric determination of methyl parathion using ZrO_2-nanoparticles modified carbon paste electrode, J. Hazard. Mater. 177 (2010) 1077–1084.
[34] M. Pirsaheb, N. Fattahi, M. Shamsipur, Determination of organophosphorous pesticides in summer crops using ultrasound-assisted solvent extraction followed by dispersive liquid-liquid microextraction based on the solidification of floating organic drop, Food Control 34 (2013) 378–385.
[35] M.A. Farajzadeh, M.R. Afshar Mogaddam, S. Rezaee Aghdam, N. Nouri, M. Bamorrowat, Application of elevated temperature–dispersive liquid–liquid microextraction for determination of organophosphorus pesticides residues in aqueous samples followed by gas chromatography–flame ionization detection, Food Chem. 212 (2016) 198–204.
[36] J.-W. Li, Y.-L. Wang, S. Yan, X.-J. Li, S.-Y. Pan, Molecularly imprinted calixarene fiber for solid-phase microextraction of four organophosphorous pesticides in fruits, Food Chem. 192 (2016) 260–267.
[37] S. Mahpishanian, H. Sershti, M. Baghdadi, Superparamagnetic core-shells anchored onto graphene oxide grafted with phenylethyl amine as a nano-adsorbent for extraction and enrichment of organophosphorus pesticides from fruit, vegetable and water samples, J. Chromatogr. A 1406 (2015) 48–58.
[38] M. Florea-Spiroiu, D. Bala, A. Balan, C. Nichita, I. Stamatin, Alginate matrices prepared in sub and supercritical CO_2, Digest J. Nanomate. Biostruct. 7 (2012) 1549–1555.
[39] J. Zhang, S. Xu, S. Zhang, Z. Du, Preparation and characterization of tamarind gum/sodium alginate composite gel beads, Iran. Polym. J. 17 (2008) 899–906.
[40] B. Sarmento, D. Ferreira, F. Veiga, A. Ribeiro, Characterization of insulin-loaded alginate nanoparticles produced by ionotropic pre-gelation through DSC and FTIR studies, Carbohydr. Polym. 66 (2006) 1–7.
[41] S. Jana, M.K. Trivedi, R.M. Tallapragada, A. Branton, D. Trivedi, G. Nayak, R.K. Mishra, characterization of physicochemical and thermal properties of chitosanand sodium alginate after biofield treatment, Pharmaceut. Anal. Acta 6 (2015) 100430.
[42] T.S. Pathak, J.S. Kim, S.-J. Lee, D.-J. Baek, K.-J. Paeng, Preparation of alginic acid and metal alginate from algae and their comparative study, J. Polym. Environ. 16 (2008) 198–204.
[43] A.B. Ross, C. Hall, K. Anastasakis, A. Westwood, J.M. Jones, R.J. Crewe, Influence of cation on the pyrolysis and oxidation of alginates, J. Anal. Appl. Pyrolysis 91 (2011) 344–351.
[44] A. Verma, M. Sharma, N. Verma, J.K. Pandit, Floating alginate beads: studies on formulation factors for improved drug entrapment efficiency and in vitro release, FARMACIA 61 (2013) 143–161.
[45] B. Mandal, K.S. Alexander, A.T. Riga, Evaluation of the drug-polymer interaction in calcium alginate beads containing diflunisal, Pharmazie 65 (2010) 106–109.
[46] Y.-F. Lin, J.-H. Chen, S.-H. Hsu, H.-C. Hsiao, T.-W. Chung, K.-L. Tung, The synthesis of Lewis acid ZrO_2 nanoparticles and their applications in phospholipid adsorption from Jatropha oil used for biofuel, J. Colloid Interface Sci. 368 (2012) 660–662.
[47] Z.-G. Shi, Y.-Q. Feng, L. Xu, M. Zhang, S.-L. Da, Preparation and evaluation of zirconia-coated silica monolith for capillary electrochromatography, Talanta 63 (2004) 593–598.
[48] T. Harnsilawat, R. Pongsawatmanit, D.J. McClements, Characterization of β-lactoglobulin-sodium alginate interactions in aqueous solutions: a calorimetry, light scattering, electrophoretic mobility and solubility study, Food Hydrocol. 20 (2006) 577–585.
[49] H. Bagheri, O. Rezvani, S. Banihashemi, Core–shell electrospun polybutylene terephthalate/polypyrrole hollow nanofibers for micro-solid phase extraction, J. Chromatogr. A 1434 (2016) 19–28.
[50] S. Mahpishanian, H. Sereshti, Three-dimensional graphene aerogel-supported iron oxide nanoparticles as an efficient adsorbent for magnetic solid phase extraction of organophosphorus pesticide residues in fruit juices followed by gas chromatographic determination, J. Chromatogr. A 1443 (2016) 43–53.
[51] R. Su, D. Li, X. Wang, H. Yang, X. Shi, S. Liu, Determination of organophosphorus pesticides in ginseng by carbon nanotube envelope-based solvent extraction combined with ultrahigh-performance liquid chromatography mass spectrometry, J. Chromatogr. B 1022 (2016) 141–152.
[52] Z. Xiao, M. He, B. Chen, B. Hu, Polydimethylsiloxane/metal-organic frameworks coated stir bar sorptive extraction coupled to gas chromatography-flame photometric detection for the determination of organophosphorus pesticides in environmental water samples, Talanta 156–157 (2016) 126–133.
[53] L. Jiang, T. Huang, S. Feng, J. Wang, Zirconium(IV) functionalized magnetic nanocomposites for extraction of organophosphorus pesticides from environmental water samples, J. Chromatogr. A 1456 (2016) 49–57.